Available online at www.sciencedirect.com
SCIENCE DIRECT®
International Journal of Solids and Structures 42 (2005) 5715–5733
INTERNATIONAL JOURNAL OF SOLIDS and STRUCTURES
www.elsevier.com/locate/ijsolstr

Numerical modelling of behaviour of reinforced concrete columns in fire and comparison with Eurocode 2

Sebastjan Bratina, Bojan Čas, Miran Saje *, Igor Planinc

University of Ljubljana, Faculty of Civil and Geodetic Engineering, Jamova 2, SI-1115 Ljubljana, Slovenia

Received 2 April 2004
Available online 14 April 2005

Abstract

The paper describes a two-step finite element formulation for the thermo-mechanical non-linear analysis of the behaviour of the reinforced concrete columns in fire. In the first step, the distributions of the temperature over the cross-section during fire are determined. In the next step, the mechanical analysis is made in which these distributions are used as the temperature loads. The analysis employs our new strain-based planar geometrically exact and materially non-linear beam finite elements to model the column. The results are compared with the measurements of the full-scale test on columns in fire and with the results of the European building code EC 2. The resistance times of the present method and the test were close. It is also noted that the building code EC 2 might be non-conservative in the estimation of the resistance time.

Keywords: Fire resistance; Finite element method; Reinforced concrete column; Thermal strain; Creep strain; Transient strain; Eurocode 2

1. Introduction

The fire resistance analysis of reinforced concrete structures constitutes an important part in their design. In the analysis an engineer usually employs various formulae for the fire resistance of structures offered by building codes, without really understanding the thermo-mechanical behaviour of a structure during fire.

* Corresponding author. Tel.: +386 1 4768 613; fax: +386 1 4768 629.
E-mail address: msaje@fgg.uni-lj.si (M. Saje).

0020-7683/$ - see front matter
doi:10.1016/j.ijsolstr.2005.03.015

Much about the behaviour of a structure in fire may be found out experimentally. The experiments are performed in specially designed furnaces in which the temperature of the surrounding air changes with time according to the prescribed law. Due to reasons of economy the furnaces are often small, so that the majority of experiments have to be limited to testing of single structural elements of small to medium size, e.g. reinforced or prestressed simply supported or continuous beams (Lin et al., 1988) and columns (Lin et al., 1992). Such a method is time consuming and the scatter of results can be wide, so that only if the number of specimens is sufficiently large, the results are statistically reliable, which makes the experiment expensive. The experiments often give a rather good picture of the overall behaviour of the structure, particularly its resistance time and the deformed shape, but cannot directly provide several other data, such as, e.g. stress distributions or transient strains during fire, which are also important for an engineer to understand the behaviour of the structure. Such data can be provided by the numerical models if they are sufficiently accurate.

To overcome these drawbacks, a considerable amount of research has been directed towards the development of numerical methods which enable the behaviour of a structure to be predicted by much less expensive computer simulations. An example of the simulations is the problem of the decision whether it is more advisable to demolish and rebuild than to repair the building which has sustained a fire (Cioni et al., 2001). The numerical analysis of the behaviour of a structure in fire requires the deduction of a firm theoretical model of the interaction between the fire and the structure which is a very complex task. A number of simplified models for the evaluation of the fire resistance of simple reinforced concrete structures have already been presented (e.g. Dotreppe et al., 1999; Eurocode 2, 2002; Lie and Celikkol, 1991), as well as the more advanced models which account for the non-linear behaviour of material in fire (Dotreppe et al., 1999; Ellingwood and Lin, 1991; Eurocode 2, 2002; Huang et al., 1999; Lie and Irwin, 1993; Sidibé et al., 2000; Zha, 2003). These models use the simplification of dividing the interaction between the fire and the structure into three separate consecutive steps. In the first step, we estimate the changing of the surrounding air temperature with time (the 'fire scenario'). In the second step, we determine the changing of temperature with time in the concrete structure as the result of the time and space dependent heat transfer from hot air into the structure. We have to perform a transient thermal analysis of the structure in which the heat conduction problem is solved, which is governed by the partial differential equation of the heat conduction, often augmented by the moister and pressure terms and equations. The effects of the heat radiation and the heat convection from air to the structure surface are accounted for via the boundary conditions. The final step consists of the determination of the time dependent (but with inertial forces disregarded) mechanical response of the structure due to the simultaneous actions of mechanical and temperature loads. The advanced non-linear mechanical models based on the 3D continuum finite element method would be perfect for this task. Unfortunately, such models are computationally too demanding for the analysis of skeletal buildings and are at present limited to the prediction of the fire response of only simple concrete members or their details. For the practical work and parametric studies, the simplified models which are based on beam and plate theories need be used, as in Cai et al. (2003); Lie and Irwin (1993); Sidibé et al. (2000). This is also the approach followed in the present paper.

We are particularly interested in the behaviour of a reinforced concrete column in fire, because columns are fundamental for the bearing capacity of skeletal structures. The deformation of the column exhibits geometrical effects such as buckling, and material effects such as progressive material softening with the temperature rise, spread of the yield through the cross-section and the redistribution of stresses in axial and cross-sectional directions (Najjar and Burgess, 1996). Thus, the fire analysis of columns represents a severe test of the accuracy of a numerical formulation. Our goal is to show that a beam-based model, when appropriately deduced, gives sufficiently reliable results for the resistance time when applied in the fire analysis of reinforced concrete columns. We prove this by comparing experimental, numerical and building code (Eurocode 2, 2002) results. We also show that the Eurocode 2 results for the fire

resistance time of reinforced concrete columns could be non-conservative. But let us first describe how the fire resistance of the reinforced concrete column is estimated by the European building code (Eurocode 2, 2002)!

2. The method for assessing the fire resistance time of reinforced concrete columns according to the European standard (Eurocode 2, 2002)

The 'standard fire resistance' is defined as the ability of a structure or its part to keep the bearing capacity during a standard fire exposure, for a specified standard period of time such as 30, 60 or 90 min. The standard fire exposure is described by an increasing temperature–time curve of the surrounding air as experienced in typical hydrocarbon fires. The temperature–time curve given in Eurocode 1 (1995) reads

$$T(t) = 20 + 345\,\log_{10}(8t + 1), \tag{1}$$

where T [°C] is the gas temperature in the fire compartment at time t [min] (see Fig. 10(a)). Eurocode 2 (2002) gives a simple formula for the fire resistance time of the reinforced concrete column subjected mainly to compression and being a member of a non-sway structure. This formula reads

$$R = 120\left(\frac{R_{\eta\mathrm{fi}} + R_a + R_l + R_b + R_n}{120}\right)^{1.8} \quad [\mathrm{min}], \tag{2}$$

where

$$\begin{aligned} R_{\eta\mathrm{fi}} &= 83\left[1 - \mu_{\mathrm{fi}}\frac{\omega + 1}{\omega + \frac{0.85}{\alpha_{\mathrm{cc}}}}\right], \\ R_a &= 1.6(a - 30), \\ R_l &= 9.6(5 - l_{0,\mathrm{fi}}), \\ R_b &= 0.09b', \\ R_n &= \begin{cases} 0 & \text{for } n = 4 \text{ (corner bars only)}, \\ 12 & \text{for } n > 4. \end{cases} \end{aligned} \tag{3}$$

The reduction factor for the design load level in fire, μ_{fi}, is determined by the equation

$$\mu_{\mathrm{fi}} = \frac{N_{\mathrm{Ed,fi}}}{N_{\mathrm{Rd}}}, \tag{4}$$

where $N_{\mathrm{Ed,fi}}$ is the design axial load in fire, and N_{Rd} is the design resistance of the column at room temperature. N_{Rd} is calculated by the use of Eurocode 2 (1991) with the partial safety factor γ_m for the room temperature design including the second-order geometrical effects with the initial eccentricity being equal to the eccentricity of $N_{\mathrm{Ed,fi}}$.

The remaining parameters in Eq. (3) are: a [mm] is the axis distance to the longitudinal steel bars; $l_{0,\mathrm{fi}}$ [m] is the effective (buckling) length of the column exposed to fire; $b' = 2A_c/(b + h)$ [mm] for the rectangular

cross-section whose sides are b and h and A_c is its area; $\omega = A_s f_{yd}/A_c f_{cd}$ denotes the reinforcement ratio at room temperature, with A_s, f_{yd} and f_{cd} being the area of the steel bars, the yield strength of steel and the compression strength of concrete, respectively; and α_{cc} is the coefficient which accounts for the reduction of compressive strength of concrete ($\alpha_{cc} = 0.85$) (Eurocode 2, 1991).

3. The thermo-mechanical response and the fire resistance time of a reinforced concrete structure in fire: The description of the computational model

The present thermo-mechanical analysis of reinforced concrete planar beam structures consists of consecutive separate thermal and mechanical time-dependent analyses. In the thermal analysis, we assume that the temperature of the surrounding air is a prescribed function of time. We further assume that the air temperature is spatially homogeneous. Then the heat transfer in the longitudinal direction of the beam can be neglected, and the 2D thermal transient analysis over only a typical cross-section of the beam is sufficient to determine the temperature distribution in the whole beam during fire. Note that the temperature determined in such a way changes across the section in a very general way. Because we deal with the planar deformations only, we here assume that the cross-section is symmetrical with respect to the plane of deformation, so that temperature is also distributed over the section in a symmetrical way. Both the temperature and its gradient are important in the mechanical analysis; the former dictates the values of material moduli, while the latter implies the temperature–driven stresses. In order to obtain the temperature and its gradients with the sufficient accuracy, the cross-section has to be modelled in the thermal analysis with a relatively dense finite-element mesh. We note in passing that the linear variation of the temperature across the section is often sufficient in the fire analysis of steel structures, see, e.g. Zhao (2000). The steel bars occupy only a small portion of the section and were therefore disregarded in the thermal analysis. Lie and Irwin (1993) show that the differences in temperature in the concrete and in the embedded steel bar at the contact are small. The temperature in the steel bar is therefore assumed as being that of concrete at its location. We also disregard the moisture transport and its evaporation and condensation in concrete, although the effect of moisture distribution histories may be significant, particularly for a higher initial moisture content. Here we assume that this is not the case. Then the flame emissivity of fire, ε_r, may have more significant effect than the moisture, which can thus safely be ignored (see Figs. 8–10 in Huang et al., 1996). The effect of moisture, on the other hand, can be very important in high strength concretes where the build-up of the high pore pressure during heating may cause the spalling of concrete, which results in the loss of strength of concrete, and in the increase of the transfer of heat to the inner layers of the section (Kodur et al., 2004). The spalling, however, does not seem to be influential enough for the normal strength concrete studied here to be considered.

Once the time-changing distribution of the temperature over the cross-section has been determined, it is imposed on a planar beam as a thermal load. Along with the self weight of the structure and additional forces required by the design rules, these loads constitute the time-dependent loading set of the structure. We use our novel finite element formulation to determine the mechanical response of the planar frame (Bratina et al., 2003a,b, 2004). The formulation is based on the modified Hu–Washizu functional of the kinematically exact planar beam theory of Reissner (1972). The only unknown functions in the functional, the extensional strain, ε, and the pseudo-curvature, κ, are approximated by the Lagrangian interpolation scheme. The remaining unknown functions, i.e. displacements, the rotation and the internal forces and moments, appear in the functional only through their boundary values. Our finite elements differ to the established ones also because they enforce the constitutive and equilibrium internal forces to be equal at the integration points (Vratanar and Saje, 1998). We use the fibre-based constitutive equations. We assume the conformity of extensional strains of concrete and steel at their contact. Note that our formulation

assumes exact kinematical equations of the beam and is thus not only materially, but also geometrically non-linear in an exact sense. The theoretical basis of the formulation and its finite element implementation details have already been described to some extent (Bratina et al., 2003a,b, 2004; Planinc et al., 2001) and a large number of the check-analyses have been performed by now proving high accuracy, economy and robustness of the formulation at room as well as at high temperatures. That is why we here present only those details that are relevant to the present discussion. The material models used in the analysis are described in Section 3.2.

3.1. The system of discretized equations of the structure

The system of the discretized equations of the structure takes the form $\boldsymbol{G}(\boldsymbol{x}, \lambda, T, t) = \boldsymbol{0}$ where $\boldsymbol{G}$ denotes the non-linear algebraic vector function of the nodal unknowns, $\boldsymbol{x}$, the mechanical loading factor, λ, the temperature, T, and time, t. It is solved by Newton's incremental–iterative method. The solution time interval is divided into time steps $[t^j, t^{j+1}]$, $j = 0, 1, \ldots$ In each step $j+1$, the mechanical loading factor increment, $\Delta\lambda$, and the temperature increment, ΔT, are prescribed, and the iterative ($i = 0, 1, 2, \ldots, n$) corrections of the unknowns of the problem, $\delta\boldsymbol{x}_{i+1}^{j+1}$, are determined by Newton's method from the system of the linearized discretized equations

$$\nabla_x \boldsymbol{G}(\boldsymbol{x}^j + \Delta\boldsymbol{x}_i^{j+1}, \lambda^{j+1}, T^{j+1}, t^{j+1})\delta\boldsymbol{x}_{i+1}^{j+1} = -\boldsymbol{G}(\boldsymbol{x}^j + \Delta\boldsymbol{x}_i^{j+1}, \lambda^{j+1}, T^{j+1}, t^{j+1}) \tag{5}$$

where $\nabla_x \boldsymbol{G} \equiv \boldsymbol{K}_{Ti}^{j+1}$ is the current tangent stiffness matrix of the structure. The values of the unknowns at the end of time step $[t^j, t^{j+1}]$ are determined by the equation

$$\boldsymbol{x}^{j+1} = \boldsymbol{x}^j + \sum_{i=0}^{n} \delta\boldsymbol{x}_{i+1}^{j+1}.$$

When the tangent stiffness matrix becomes singular ($\det\boldsymbol{K}_{Ti} = 0$), the structure reaches its critical state which is either the limit or the bifurcation point. This state is described by the quadruple $\boldsymbol{x}_{\mathrm{cr}}$, λ_{cr}, T_{cr}, and t_{cr}, and is assumed to represent the bearing capacity of the structure (the collapse). The related time and the related temperature are termed the 'fire resistance time' and the 'critical temperature'. During a typical fire analysis, the mechanical loading factor is kept constant ($\lambda = \text{const.}$), while the temperature rises until the collapse takes place at the critical temperature. The singularity of the tangent stiffness matrix indicates the global instability of the structure. In addition to the global instability, the local instability may take place during fire. This is defined as the state at which the determinant of the tangent constitutive matrix of a cross-section becomes zero (Bratina et al., 2003a, 2004). Once the tangent constitutive matrix becomes singular, the cross-section experiences the strain-softening in the subsequent progressive deformation while its neighbouring cross-sections have to start the unloading. If strained in the softening regime, the cross-section is unstable. When the structure is statically determinant and if the geometrically non-linear effect is not dominant, the local instability of the cross-section instantaneously causes the global instability of the structure. Notice that concrete has a relatively large strain-softening capability, in particular at high temperatures, so both mechanisms of the instability have been considered in our formulation.

Remark. The critical temperature (or the collapse) may be defined in various ways. One of the more popular conditions is that the maximum displacement in the structure reaches a prescribed large value. Note that this condition and the $\det\boldsymbol{K}_T = 0$ condition employed here do not yield the same result for the critical temperature.

3.2. Mechanical properties of concrete and steel. Strain and stress increments

The geometric, i.e. total extensional strain increment ΔD of a generic material fibre is assumed to be the sum of increments of elastic, ΔD_e, plastic, ΔD_p, thermal, ΔD_{th}, creep, ΔD_{cr}, and transient strain increment, ΔD_{tr}, the latter being non-zero in concrete and vanishing in steel:

$$\Delta D = \Delta D_e + \Delta D_p + \Delta D_{th} + \Delta D_{cr} + \Delta D_{tr}. \tag{6}$$

The sum of elastic and plastic parts of the strain will be termed the mechanical strain, $D_\sigma = D_e + D_p$. We assume that the relationship between the mechanical part and the longitudinal normal stress, σ, is given by the constitutive law $\sigma = \mathscr{F}(D_\sigma, T)$, where $\mathscr{F}$ is a functional pertinent to the chosen material. In the present fire analysis, we use the constitutive laws of concrete and reinforcing steel as suggested by Eurocode 2 (2002). The graphs of the relationships are depicted in Fig. 1. The figure puts it clear that the increase in temperature decreases the strength of material and increases its ductility. Both materials, concrete and steel, exhibit the extensive strain-softening in the post-strength regime. Once functional $\mathscr{F}$ is given, the stress increment $\Delta\sigma^{j+1}$ in the time step $[t^j, t^{j+1}]$ is given by the relation $\Delta\sigma^{j+1} = \sigma^{j+1} - \sigma^j = \mathscr{F}(D_\sigma^{j+1}, T^{j+1}) - \mathscr{F}(D_\sigma^j, T^j)$. The unloading is assumed as being elastic with an elastic modulus taken at the current temperature. An isotropic model of the strain-hardening is assumed in the loading–unloading cycles.

The thermal strain in concrete, $D_{th,c}$, is assumed to be a function of the current temperature and is given by the relation $D_{th,c} = \tau(T)$. The approximation of functional τ is defined in Eurocode 2 (2002) and is also adopted here. The thermal strain increment in time step $[t^j, t^{j+1}]$ is thus determined by the equation $\Delta D_{th,c}^{j+1} = \tau(T^{j+1}) - \tau(T^j) = D_{th,c}^{j+1} - D_{th,c}^j$.

The concrete creep strain, $D_{cr,c}$, is assumed to be a function of the current stress, time and temperature. Here we employ the model proposed by Harmathy (1993)

$$D_{cr,c}^{j+1} = \beta_1 \frac{\sigma_c^{j+1}}{f_{cT}^{j+1}} (t^{j+1})^{1/2} e^{d(T^{j+1}-293)}, \tag{7}$$

where f_{cT}^{j+1} is strength of concrete at temperature T^{j+1} [K], t^{j+1} [s] is time and β_1 [$s^{-1/2}$] and d [K^{-1}] are empirical constants of material. The least square method analysis of the data of creep tests, performed by Cruz (1968), gives $\beta_1 = 6.28 \times 10^{-6}\ s^{-1/2}$ and $d = 2.658 \times 10^{-3}\ K^{-1}$. Fig. 2 shows the comparisons between the experimental and analytical results using (7) for creep strains at various temperatures in the range from 24 °C to 649 °C. Note that the agreement is satisfactory.

The creep strain increment $\Delta D_{cr,c}^{j+1}$ in time step $[t^j, t^{j+1}]$ is given by the equation $\Delta D_{cr,c}^{j+1} = D_{cr,c}^{j+1} - D_{cr,c}^j$.

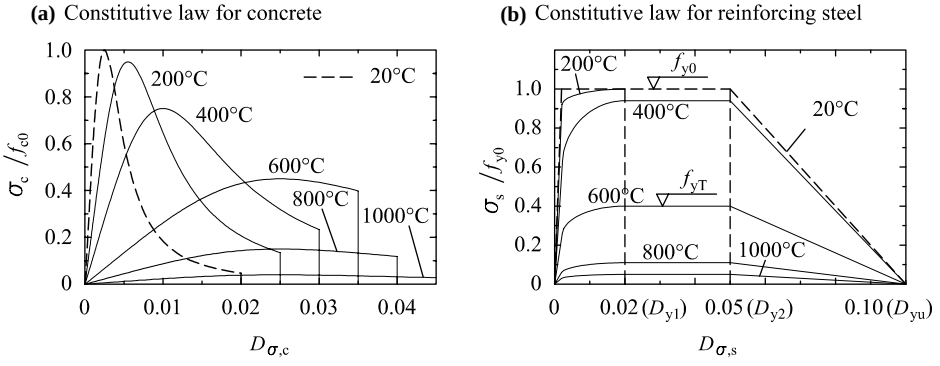

Fig. 1. Constitutive laws for concrete and reinforcing steel according to Eurocode 2 (2002).

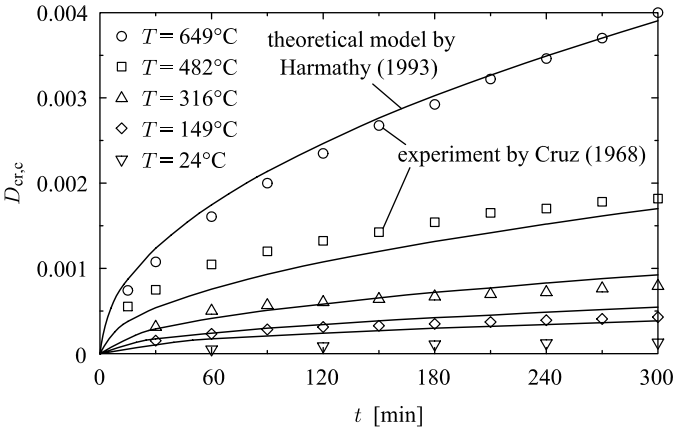

Fig. 2. The variations of creep strain with time according to the model proposed by Harmathy (1993) and the experimental data by Cruz (1968).

The transient strain in concrete ($D_{tr,c}$) has been found to have an important influence on mechanical behaviour of concrete during the first heating of concrete (see Anderberg and Thelandersson, 1976). It is irrecoverable and is the result of the physico-chemical changes that take place only under the first heating. Formally, it may be defined as the part of the total strain obtained in stressed concrete under heating that cannot be accounted for otherwise. In our formulation we use the transient strain model of Anderberg and Thelandersson (1976)

$$\Delta D_{tr,c}^{j+1} = k_2 \frac{\sigma_c^{j+1}}{f_{c0}} \Delta D_{th,c}^{j+1}, \tag{8}$$

where f_{c0} is strength of concrete at the room temperature; k_2 is a dimensionless constant whose value ranges from 1.8 to 2.35. This model assumes that the change of the transient strain is linearly dependent on the change of the current thermal strain.

The thermal strain of steel, $D_{th,s}$, is assumed to be a function of the current temperature, see Eurocode 2 (2002). Accordingly, the thermal strain increment in steel is determined by the equation $\Delta D_{th,s}^{j+1} = D_{th,s}^{j+1} - D_{th,s}^{j}$.

The creep strain of steel ($D_{cr,s}$) becomes considerable when the temperature of steel exceeds 400 °C. There is a number of creep models available for steel at high temperature. In our research we employ the model proposed by Williams-Leir (1983). This model assumes that the creep strain is a function of the current stress and temperature in steel, and that its evolution in time is governed by the differential equation

$$\dot{D}_{cr,s} = \mathrm{sgn}(\sigma_s) b_1 \coth^2(b_2 |D_{cr,s}|). \tag{9}$$

Material parameters b_1 and b_2 are the functions of stress and temperature in steel, see Williams-Leir (1983). Even if we assume that σ_s and T are given functions of time, Eq. (9) is a complicated differential equation that needs to be integrated numerically. Here we employ the iterative solution method in which the time derivative is substituted by the implicit differential quotient. The creep strain increment of steel in time step $[t^j, t^{j+1}]$ is thus determined by the equation

$$\Delta D_{cr,s}^{j+1} = \mathrm{sgn}(\sigma_s^{j+1}) b_1 \coth^2(b_2 |D_{cr,s}^{j+1}|) \Delta t^{j+1}. \tag{10}$$

The flowchart of the incremental-iterative solution procedure of the mechanical response of the structure is given in Box 1.

Box 1: Flowchart of the incremental–iterative solution procedure.

TIME STEP $[t^j, t^{j+1}]$:

$$t^{j+1} = t^j + \Delta t^{j+1}, \quad T^{j+1} = T^j + \Delta T^{j+1}, \quad \lambda^{j+1} = \lambda^j + \Delta\lambda^{j+1}, \quad \Delta D^{j+1}_{\mathrm{th,c}(s)} = D^{j+1}_{\mathrm{th,c}(s)} - D^{j}_{\mathrm{th,c}(s)}.$$

[◊] **Structure level**: Newton's iterative method ($i = 0,1,2,\ldots$): $\nabla_{\boldsymbol{x}}\boldsymbol{G}\delta\boldsymbol{x}^{j+1}_{i+1} = -\boldsymbol{G}$.

[•] **Element level**:

[○] Initialization: $\Delta\boldsymbol{x}^{j+1}_{i=0} = 0$.

[○] For all integration points $(y_{\mathrm{c}}, z_{\mathrm{c}})$ of the concrete cross-section at quadrature points x_q: Newton's iterative solution of $\Delta\sigma^{j+1}_{c,i}$, $\Delta D^{j+1}_{cr,c,i}$ and $\Delta D^{j+1}_{\mathrm{tr,c},i}$:

$$F_1 = \Delta\sigma^{j+1}_{\mathrm{c},i} - \mathscr{F}(D^{j+1}_{\sigma,\mathrm{c},i}, T^{j+1}) - \mathscr{F}(D^{j}_{\sigma,\mathrm{c},i}, T^{j}) = 0,$$

$$F_2 = \Delta D^{j+1}_{\mathrm{cr,c},i} - D^{j+1}_{\mathrm{cr,c},i} + D^{j}_{\mathrm{cr,c},i} = 0,$$

$$F_3 = \Delta D^{j+1}_{\mathrm{tr,c},i} - k_2\frac{\sigma^{j+1}_{\mathrm{c},i}}{|f_{\mathrm{c}0}|}\Delta D^{j+1}_{\mathrm{th,c},i} = 0.$$

[○] For all reinforcing bars $(y^k_{\mathrm{s}}, z^k_{\mathrm{s}})$ in the cross-section at x_q: Newton's iterative solution of $\Delta\sigma_{\mathrm{s},i}{}^{j+1}$ and $\Delta D^{j+1}_{\mathrm{cr,s},i}$:

$$F_4 = \Delta\sigma^{j+1}_{\mathrm{s},i} - \mathscr{G}(D^{j+1}_{\sigma,s,i}, T^{j+1}) - \mathscr{G}(D^{j}_{\sigma,\mathrm{s},i}, T^{j}) = 0,$$

$$F_5 = \Delta D^{j+1}_{\mathrm{cr,s},i} - \mathrm{sgn}(\sigma^{j+1}_{\mathrm{s},i})b_1\coth^2(b_2|D^{j+1}_{\mathrm{cr,s},i}|)\Delta t^{j+1} = 0.$$

[○] Compute $\mathscr{N}^{j}_{\mathrm{c},i}$, $\mathscr{M}^{j}_{\mathrm{c},i}$ and the contribution of the cross-section to the tangent stiffness matrix and the loading vector of the element.

[○] Compute the tangent stiffness matrix of the element, $\boldsymbol{K}_{\mathrm{el}}$, and the corresponding loading vector, $\boldsymbol{G}_{\mathrm{el}}$:

$$\boldsymbol{K}_{\mathrm{el}}(\boldsymbol{x}^j + \Delta\boldsymbol{x}^{j+1}_i, \lambda^{j+1}, T^{j+1}, t^{j+1}),$$

$$\boldsymbol{G}_{\mathrm{el}}(\boldsymbol{x}^j + \Delta\boldsymbol{x}^{j+1}_i, \lambda^{j+1}, T^{j+1}, t^{j+1}).$$

[•] Compute the tangent stiffness matrix of the structure, $\boldsymbol{K}_T = \nabla_{\boldsymbol{x}}\boldsymbol{G}$, and the corresponding loading vector, $\boldsymbol{G}$:

$$\boldsymbol{K}_T(\boldsymbol{x}^j + \Delta\boldsymbol{x}^{j+1}_i, \lambda^{j+1}, T^{j+1}, t^{j+1}),$$

$$\boldsymbol{G}(\boldsymbol{x}^j + \Delta\boldsymbol{x}^{j+1}_i, \lambda^{j+1}, T^{j+1}, t^{j+1}).$$

[•] Compute the corrections of displacement increments:

$$\delta\boldsymbol{x}^{j+1}_{i+1} = -\boldsymbol{K}^{-1}_T\,\boldsymbol{G},$$

$$\Delta\boldsymbol{x}^{j+1}_{i+1} = \Delta\boldsymbol{x}^{j+1}_i + \delta\boldsymbol{x}^{j+1}_{i+1},$$

$$\boldsymbol{x}^{j+1}_{i+1} = \boldsymbol{x}^j + \Delta\boldsymbol{x}^{j+1}_{i+1}.$$

[◊] Stop iteration if

$$\|\delta\boldsymbol{x}^{j+1}_{i+1}\| < \text{ prescribed tolerance(typically } 10^{-8}),$$

continue otherwise.

[◊] Stop if numerical collapse of the structure is reached ('fire resistance time'):

$$\det\boldsymbol{K}_T = 0.$$

Remark. The majority of the numerical formulations of the fire analysis of the reinforced concrete structures do not differentiate between the plastic and creep strains in concrete. They employ the combined plastic strain which includes both the plastic and the creep strain parts. The stress in concrete is then taken to be a function of this combined strain (Lie and Irwin, 1993; Zha, 2003). Such a material model cannot account for the rates of temperature and creep strain properly, neither is able to divide the resulting combined plastic strain into the physical plastic and creep parts. The transient creep in concrete is usually ignored (Zha, 2003).

By contrast, the present formulation considers each of the physical strain parts separately, thus enabling an engineer to follow the time variation of each particular strain and to assess its contribution to the total strain. This holds true for both concrete and steel materials.

4. Numerical examples

4.1. Clamped reinforced concrete column

4.1.1. Comparisons with experiment (Lin et al., 1992)

In this example we compare the results of our numerical model with the experimental results of full-scale laboratory fire tests on the centrically loaded reinforced concrete column, performed by Lin et al. (1992) and reported on by Lie and Irwin (1993). The geometric and loading data are given in Fig. 3. The self-weight of the column is modelled as an axial traction. In order to simulate a fire situation, the column was exposed to hot surrounding air in such a way that the air temperature (generated by the furnace) was changing according to the ASTM fire curve (1976). The yield stress of the reinforcing bars was $f_{y0} = 42\ \mathrm{kN/cm^2}$, while the strength of siliceous aggregate concrete at room temperature was $f_{c0} = 3.61\ \mathrm{kN/cm^2}$. The measured fire resistance time of the column was 208 min (Lie and Irwin, 1993). The related critical temperature was 1087 °C.

The remaining material parameters and their temperature dependence, needed in the numerical analysis of the mechanical response, were estimated using the given strengths and the data from Eurocode 2 (2002).

In the first step, we have to determine the temperature distribution over the cross-section at discrete times t^j during fire. The 2D transient heat conduction problem was solved by our computer programme

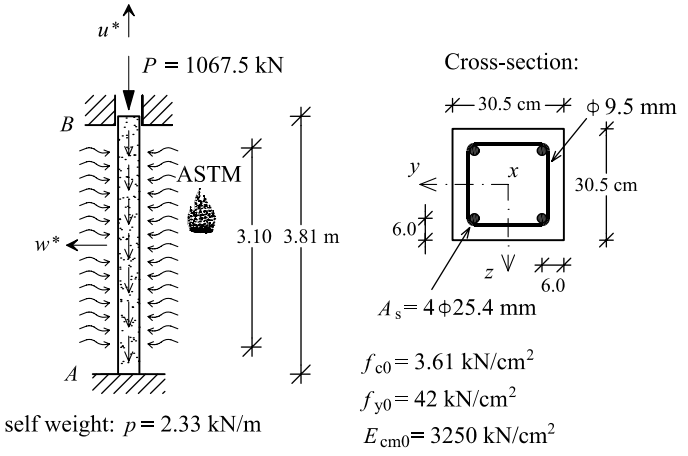

Fig. 3. Clamped centrically loaded reinforced concrete column in fire (Lin et al., 1992).

(Saje and Turk, 1987). The transfer of heat due to the radiation and the air convection at the boundaries were taken into account in a standard way. Thermal parameters, such as the conductivity k_c, the convection heat transfer coefficient h_c and the emissivity ε_r, were not presented in the report by Lie and Irwin (1993) and were hence selected in such a manner that the calculated and the measured temperatures in concrete agreed as much as possible ($\varepsilon_r = 0.3$, $h_c = 20$ W/m K, the graph of k_c is depicted in Fig. 4). The remaining parameters, needed in the analysis of the temperature field, were estimated on the basis of Eurocode 2 (2002). End parts of the column were thermally insulated, so that the actual length of the column exposed to fire was 310 cm. Fig. 5 shows the calculated and the measured temperature distributions in concrete cross-section along its centerline at various times, as well as the calculated isothermals. We see that the calculated and the measured temperatures agree well. The figure also shows the temperature distributions suggested by Eurocode 1 (1995); these distributions assume that the column is not insulated. The disagreement between the measured and the Eurocode 1 distributions is rather big. The Eurocode curves exhibit larger temperatures than the experiment at the surfaces of the cross-section, and substantially smaller temperatures at the central region of the cross-section. The calculated time-dependent temperature field varying over the cross-section was used as the thermal load of the column in the subsequent mechanical analysis.

The mechanical response of the column subjected to thermal and mechanical loads was obtained by our computer programme, made in Matlab (MathWorks, 1999). The column was modelled by six beam finite elements with ε and κ being interpolated with the Lagrangian polynomials of the fourth order. In order to initiate the buckling, the axis of the column was made imperfect with small eccentricity 0.01 cm. The cross-sectional integration needed to determine the constitutive axial force and constitutive bending moment and the cross-sectional constitutive tangent stiffness matrix was performed numerically. We used the 3×3-point Gaussian integration with the total of 180 integration points over one half of the cross-section.

Fig. 6 shows how the measured axial displacement was changing with time. We can see that the axial displacement was increasing during the first 120 min. This corresponds to the elongation of the column which is due to the growing thermal strain. Subsequently, the axial displacement started decreasing. This caused the shortening of the column which was due to the rapid increase of creep and transient strains. This kind of the behaviour is typical for the reinforced concrete columns.

We find it interesting to study the effect of individual strain parts in concrete and steel on the mechanical behaviour of the column. If only the thermal strain (D_{th}) is considered (while D_{cr} and D_{tr} neglected), the axial displacement u^* of the column becomes maximal at about 90 minutes and is greater than the measured one (see Fig. 6). This remains true if the creep strain of concrete ($D_{cr,c}$) and, particularly, the transient strain (D_{tr}) are also considered, yet the maxima are now lower and the final axial displacement at the

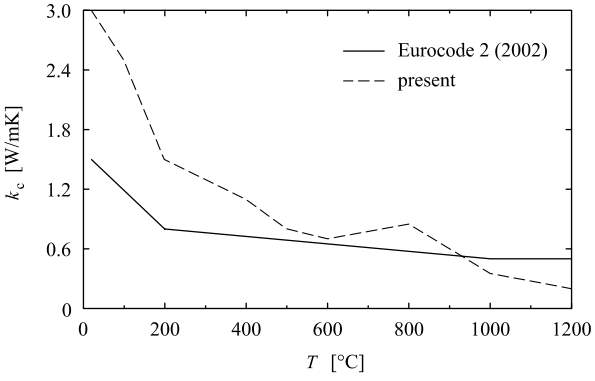

Fig. 4. The variation of conductivity k_c with temperature.

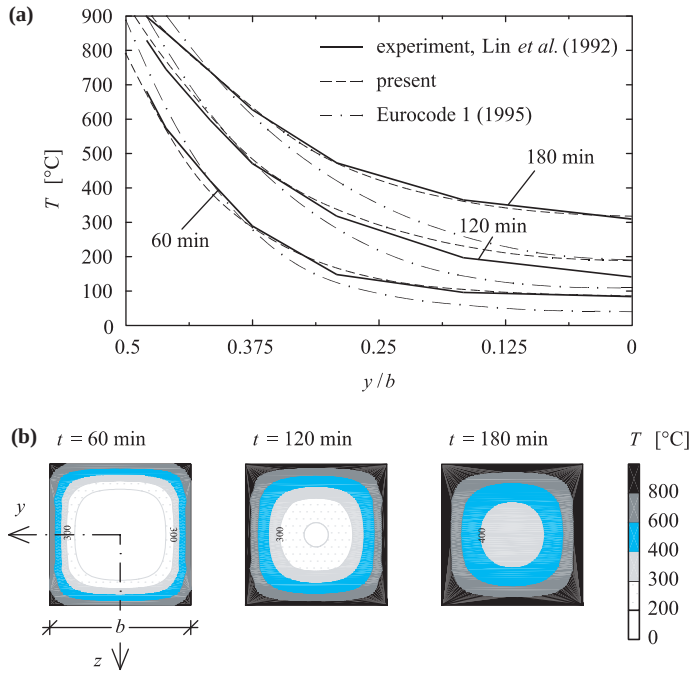

Fig. 5. Reinforced concrete column: (a) the comparison between the measured, the calculated and the Eurocode temperature distributions along the axis $z = 0$ at times 60, 120 and 180 min; (b) the calculated isothermals at times 60, 120 and 180 min.

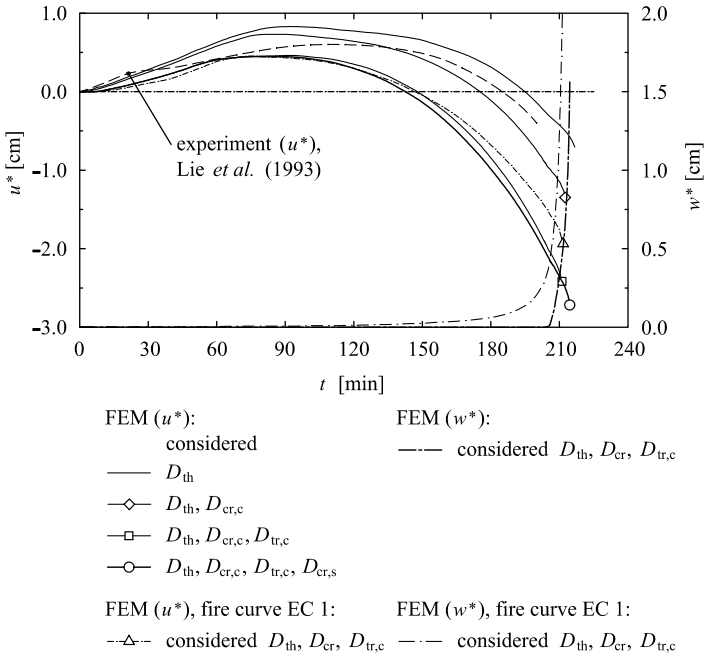

Fig. 6. Reinforced concrete column. The variation of axial displacement (u*) at point B and the lateral displacement at the mid-point of the column (w*) with time.

collapse at about 210 minutes is considerably bigger. The calculated displacement at the collapse is this time greater than the measured one, although we used the least recommended value (1.8) for the constant k_2 in the transient strain increment expression. This suggests that the specimen was probably almost dry when the test started. Consequently, the transient strain can be neglected. The creep strain in steel ($D_{cr,s}$) does not effect the axial displacement considerably (see Fig. 5), because the highest temperature in reinforcing steel is not greater than 400 °C and because steel Au 50 which is the least sensitive to creep was used.

Surprisingly, the calculated fire resistance time does not depend much on which strain parts are considered or neglected and rather well equals to the resistance time measured in experiment. Fig. 6 also shows the variation with time of the calculated lateral displacement w^* at the mid-point of the column. A sudden increase in w^* well indicates the onset of the buckling of the column at time 205 min and the subsequent critical state at about 215 min, which is close to 208 min reported in Lie and Irwin (1993). Fig. 6 further shows the results of our model when the mechanical analysis using thermal parameters according to Eurocode 1 (1995) is made (Fig. 5), and the thermal insulation at the bottom and at the top of the column is disregarded. The results for the displacements and the resistance time ($t_{cr} = 211.7$ min) do not differ essentially in comparison with the results that employed the more realistic temperature distributions. Hence, in the particular column in fire considered here, the accuracy of the temperature field was not the essential factor.

Fig. 7 shows the distribution of strains (ε, κ) along the centroidal axis of the column at $t = 90$ min and at the instant of the numerical collapse, $t_{cr} = 214.4$ min. All kinds of the strain parts were taken into account. As expected, the least values of strains appear at the top and at the bottom of the column in the insulated areas. Until the buckling starts at 205 min, the column remains straight and the pseudocurvature zero. At the critical time, $t_{cr} = 214.4$ min, when the column collapses, the longitudinal strain is still dominant, i.e. about 30-times larger than the corresponding maximal pseudocurvature. Note that the elongation at the exposed part of the column at 214.4 min is roughly 10-times bigger than at 90 min. By contrast, the elongation at the insulated parts remains practically constant.

The results of the numerical analysis make it possible to assess the contribution of individual strain parts to the integral response of the column. Fig. 8 shows the isolines of thermal, geometric, mechanical, creep and transient strains and stress in concrete at the mid-point cross-section at 180 min. At this instant the column is still unbuckled; that is why the geometrical strain is homogeneous across the section. The remaining strains vary over the cross-section. With the exception of the mechanical strain, the strains attain their

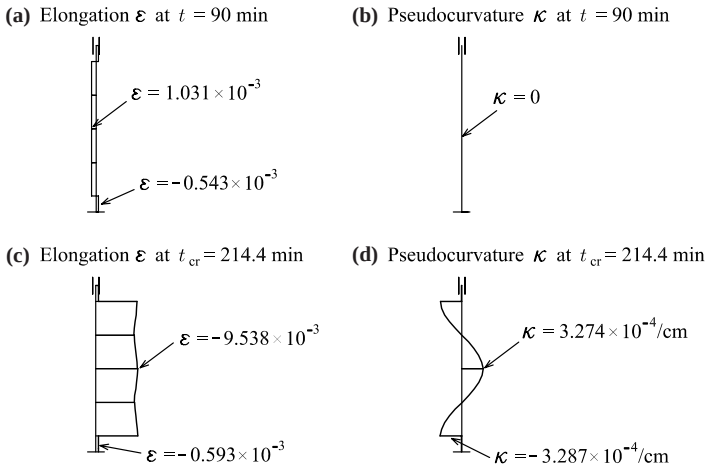

Fig. 7. Reinforced concrete column. Strain distributions along the centroidal axis of column: (a) $t = 90$ min and (b) $t_{cr} = 214.4$ min.

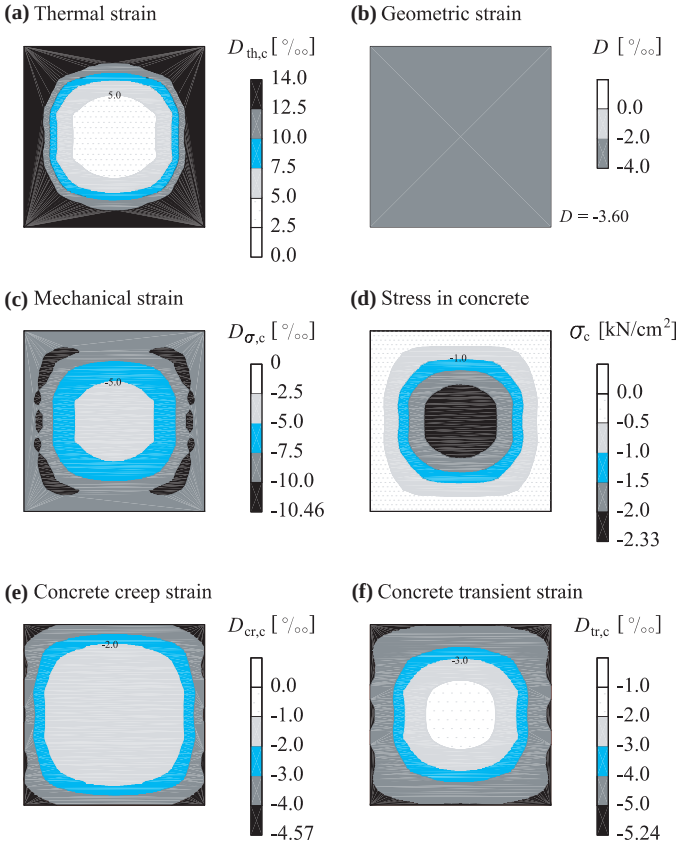

Fig. 8. Reinforced concrete column. Isolines for various strains and stress in concrete at mid-point cross-section at $t = 180$ min.

maximal values at the surface of the cross-section. Note that the concrete transient strains are comparable in size with thermal or mechanical strains. They are, however, compressive, in contrast to thermal strains which are tensile. Mechanical strains are also compressive; they are maximal at regions positioned a few centimetres away from the surface of the section. The stresses in concrete are also not homogeneous over the section. They are maximal at the centre region of the section. Fig. 8(d) shows that about one third of the section is practically not stressed at this instant.

4.1.2. Comparisons with Eurocode 2 (2002)

According to Eurocode 2, the fire resistance time of a reinforced concrete column is given by formulae (2)–(4). First, we have to calculate the design resistance of the column at room temperature. The related procedure which is well described in Eurocode 2 (1991) requires the second order effects to be included via the geometrical imperfection and prescribes different partial safety factors for action ($\gamma = 1.35$) and for material properties ($\gamma_c = 1.5, \gamma_s = 1.15$). Assuming the geometrical imperfection to be $e_a = 0.49$ cm, we obtain $N_{Rd} = 2394$ kN; the design resistance calculated by our numerical model is 2556 kN, which is about 7% larger value. The effective length of the clamped beam is $l_{0,fi} = 1.91$ m. The selected reduction factor for the design load level in fire was $\mu_{fi} = 0.446$ and $\mu_{fi} = 0.418$, respectively. Inserting these values into Eq. (2) gives $R_{EC2} = 180.8$ min (at $T_{cr} = 1110$ °C) for $N_{Rd} = 2394$ kN and $R_{EC2} = 186.7$ min (at $T_{cr} = 1115$ °C) for $N_{Rd} = 2556$ kN.

Eurocode 2 assumes that the column is not insulated, in contrast to the present column which is partly thermally insulated. In order to make a fair comparison, in our numerical calculations we also assumed that the column is not insulated. The results of the analysis are shown in Fig. 6 for displacements u^* and w^* as functions of time. The calculated resistance time is 211.7 min. This is remarkably more than the resistance time 180.8 min predicted by Eurocode 2. A similar conservativeness of Eurocode 2 with regard to the resistance time of circular reinforced concrete columns was reported by Franssen and Dotreppe (2003).

4.2. Simply supported reinforced concrete columns: Comparisons with Eurocode 2 (2002)

We study the behaviour of two simply supported perfectly straight columns, here denoted by C_1 and C_2. Both columns are subjected to a compressive axial load and bending moments at the supports. Column C_1 (height 4 m) is subjected to an eccentric axial force. We consider three different eccentricities, $e = 0$; 0.015; and 0.04 [m], and study their effect. Column C_2 (height 4.5 m) is subjected to a smaller axial force and large, but unequal boundary moments (see Fig. 9). The self weight of the columns is modelled as an axial traction. The variation of the surrounding air temperature with time is assumed after Eurocode 1 (1995) (Eq. (1)). Geometrical and mechanical data along with the load disposition are presented in Fig. 9.

The amount of the reinforcement and the design resistance of the columns were calculated according to Eurocode 2 (1991). The partial safety factors for actions and for material properties were taken to be $\gamma = 1.35$ and $\gamma_c = 1.5$, $\gamma_s = 1.15$, respectively. The resistance of column C_1 at room temperature was found to be $N_{\mathrm{Rd},C_1} = 1350$ kN for all three values of eccentricities. The related areas of the steel reinforcement are: $A_s = A'_s = 7.56$ cm^2 for $e = 0$; $A_s = A'_s = 10.68$ cm^2 for $e = 0.015$; and $A_s = A'_s = 16.04$ cm^2 for $e = 0.04$. The resistances of these columns, obtained by the present numerical method, are 1527 kN, 1451 kN and 1399 kN. These values are from 4–13% bigger than the one obtained from the code. The resistance of column C_2 at room temperature is $N_{\mathrm{Rd},C_2} = 945$ kN, $M_{\mathrm{Rd},1,C_2} = -47.3$ kN m or $M_{\mathrm{Rd},2,C_2} = 75.6$ kN m. From this $A_s = A'_s = 6.32$ cm^2 follows. The selected reduction factors for the design load level in fire were $\mu_{\mathrm{fi}} = 0.5$ and $\mu_{\mathrm{fi}} = 0.4$ for columns C_1 and C_2, respectively (see Fig. 9 and Eq. (4)). The corresponding fire resistance times by Eurocode 2 (2002) are $R_{C_1} = 123.8$ min (at $T_{\mathrm{cr}} = 1054$ °C) and $R_{C_2} = 108.7$ min (T_{cr} being 1034 °C). Note that the resistance time in Eurocode 2 does not depend on the eccentricity of the load and/or the area of the reinforcement; that is why all of the three cases of column C_1 have the same resistance time.

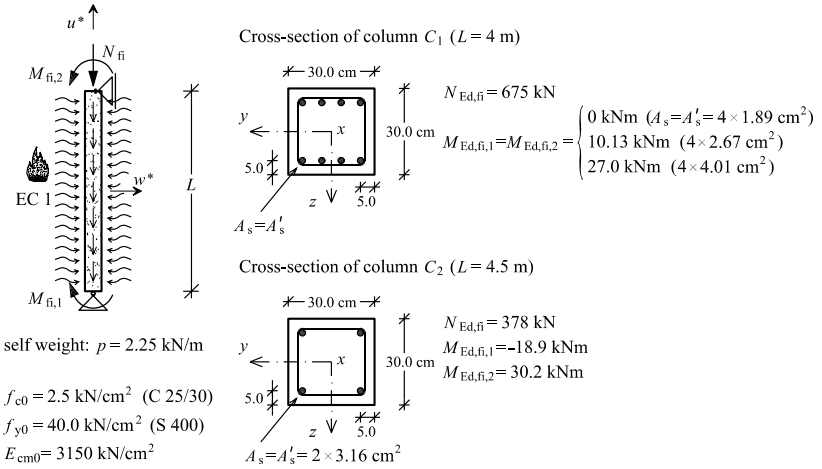

Fig. 9. The geometrical and mechanical data for eccentrically loaded reinforced concrete columns.

Thermal parameters of concrete, i.e. conductivity k_c, specific heat c_c, convection heat transfer coefficient h_c, emissivity ε_r and density ρ_c, were chosen on the basis of the data from Eurocode 2 (2002) for concrete with the siliceous aggregate and for the moisture content 1.5% of the concrete weight. The calculated temperature distributions over the cross-section (see Fig. 10) well agree with those presented in Eurocode 2 (2002). Fig. 10 also shows the changing of the temperature with time in the most and the least exposed steel bars. We can observe that the temperature in the bars is much smaller than the temperature of the surrounding air (dashed line in the figure), which is the consequence of the relatively thick concrete cover.

In the mechanical analysis, each column was modelled by six equally long beam finite elements of the fourth-order. We used Lobatto's integration for the line integrals and Gaussian integration for the cross-sectional integrals. Concrete with siliceous aggregate and the cold formed reinforcing steel were assumed to define the dependence of concrete and reinforcing steel material parameters on temperature. We assume that steel is only lightly sensitive to creeping. Constant k_2, characterizing the transient strain increment, was taken to be equal 1.8.

When disregarding creep of concrete and steel, and also transient strain in concrete, our numerical model yields the fact that the resistance time of column C_1 is practically insensitive to the eccentricity of the axial force, the resistance times of the three columns being 121.5, 117.3 and 121.3 min for $e = 0$; 0.015; and 0.04 [m]. These values are only slightly smaller than the value suggested by Eurocode 2, i.e. $R_{C_1} = 123.8$ min. The time developments of the axial and lateral displacements are displayed in Fig. 11 for all three cases. Note that column C_1 collapsed after an excessive growth of the lateral deflection.

In Section 4.1.1 we observed that the effects of creep of concrete and steel as well as the transient strains in concrete onto the fire resistance time were small. This is not true in the present case of column C_1. When

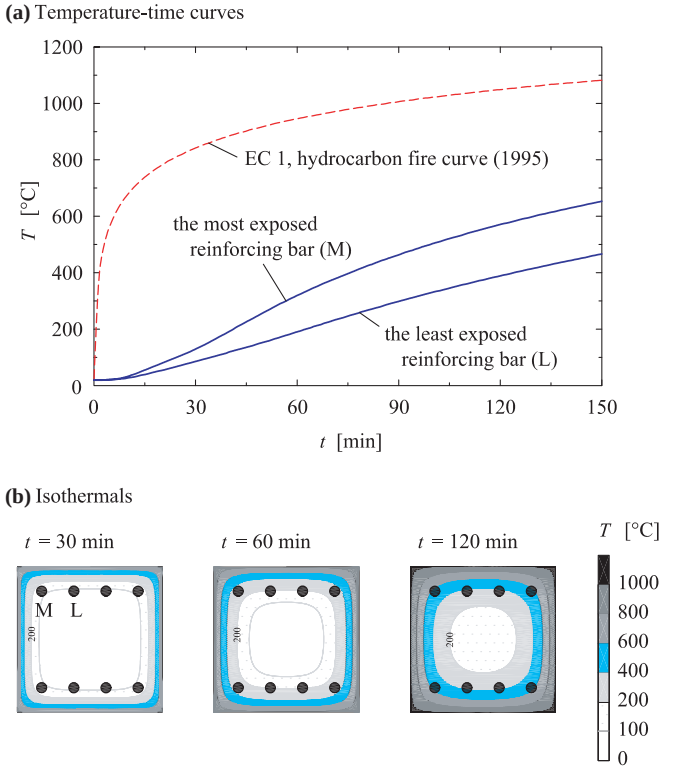

Fig. 10. Eccentrically loaded reinforced concrete columns. Temperature response.

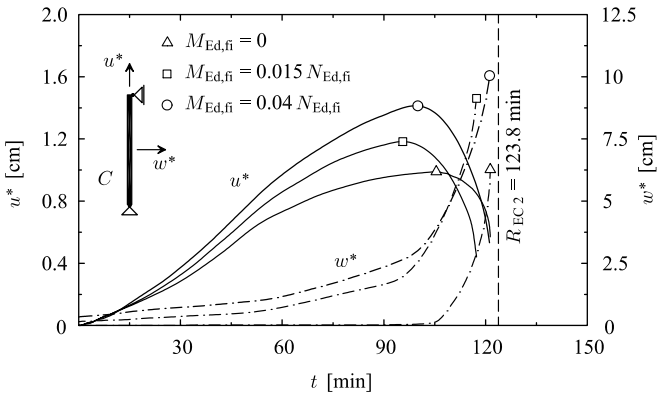

Fig. 11. Eccentrically loaded reinforced concrete column C_1. Variation of axial and lateral displacements with time. Only D_{th} considered.

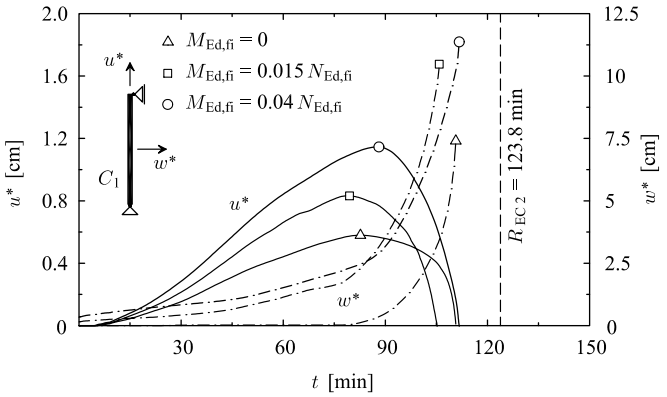

Fig. 12. Eccentrically loaded reinforced concrete column C_1. Variation of axial and lateral displacements with time. Creep and transient strain considered.

these strains are considered, the numerically found resistance times are about 10% smaller, i.e. 110.8, 106.0 and 111.7 min, respectively. Fig. 12 shows the related time graphs of the displacements. Observe that the axial displacement, u^*, increases during the first 80–90 min (reaching the value 1.15 cm for the eccentricity 4 cm), and decreases afterwards. It takes the value about 0 cm at the collapse of the column. By contrast, the lateral displacement increases all the time. A rather substantial lateral displacement may be observed at the collapse ($w^*_{cr} = 11.02$ cm for $e = 4$ cm).

The fire resistance time for column C_2, calculated by the non-linear analysis, is 102.3 min, when we disregard the creep strains in concrete and steel and the transient strains in concrete, and 92.1 min otherwise. This is 16.6 min less than the Eurocode 2 fire resistance time. Like column C_1, column C_2 failed after an excessive growth of the lateral deflection. Fig. 13 shows the variation of the axial and lateral displacements with time. When all kinds of strain contributions are considered, the axial and the lateral displacements at the collapse time are 0.78 cm and 9.48 cm, respectively.

Fig. 14 shows the deformed shapes and the distribution of bending moments $\mathscr{M}$ for the two columns at $t = 60$ min and at the time of collapse, t_{cr}. The contribution of all kinds of strain is considered. The dis-

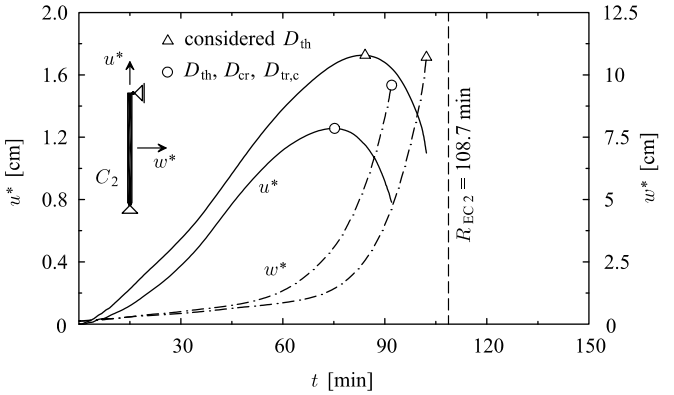

Fig. 13. Eccentrically loaded reinforced concrete column C_2. Variation of axial and lateral displacements with time. Only D_{th} (triangles) or D_{th},D_{cr},$D_{tr,c}$ (circles) considered.

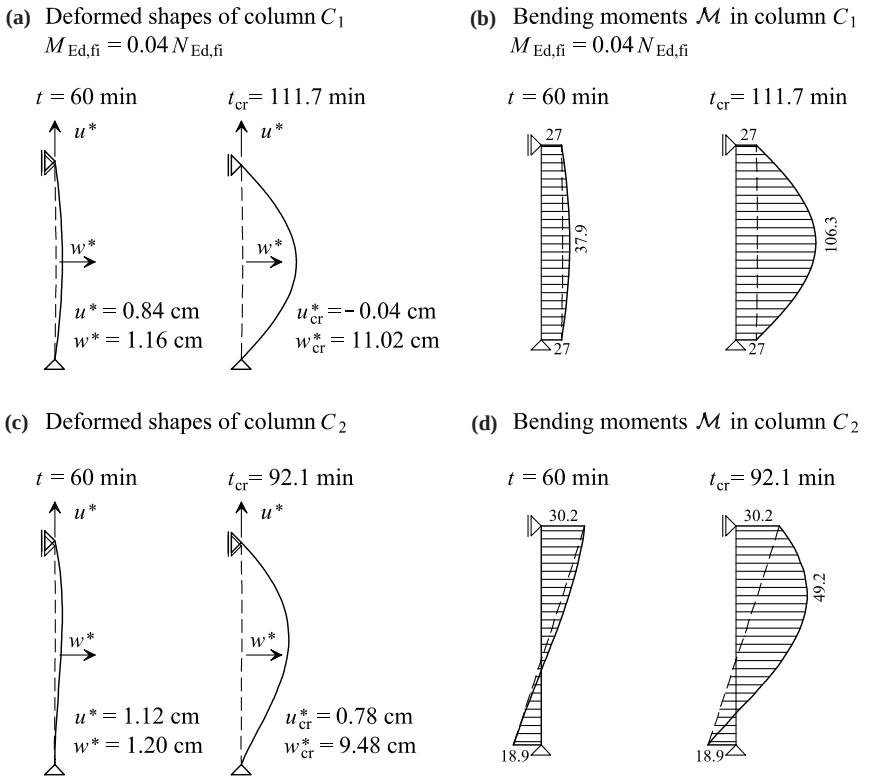

Fig. 14. Deformed shapes (10-times magnified) and distributions of bending moment for eccentrically loaded columns C_1 and C_2.

placements are 10-times magnified. The dashed curve depicts the related state of the column before the thermal load is applied. As observed from the figures, even one hour after the temperature starts increasing, the deformed shape and the distribution of the bending moment are practically unchanged. This situation changes considerably at the collapse.

5. Conclusions

We described a two-step finite element formulation for the thermo-mechanical, transient, non-linear analysis of the behaviour of the reinforced concrete columns in fire. In the first step, we determine the temperature distributions over the cross-sections of the column in fire as a function of time. These constitute the time and space dependent temperature load of the column. In the mechanical analysis, we employ our new strain-based 2D geometrically exact and materially non-linear beam finite elements to model the column. These finite elements are special because they satisfy the conditions that the equilibrium and constitutive axial forces and bending moments coincide at the integration points.

Because the thermo-mechanical processes in the column during fire are really complicated, such a beam-based analysis might seem to be too simple to predict realistic behaviour. Yet the comparison with the experiments performed by Lin et al. (1992) on clamped reinforced concrete columns, made in our first numerical example, show a very good agreement in the resistance time. The agreement in the variation of the axial displacement with time was only qualitative. The disagreement in the axial displacement indicates that the functional relations for some of the strain parts (thermal, creep, transient) or their material parameters as taken in the present study have not been modelled with a sufficient accuracy to describe the materials employed in the experiment. A further research will be needed to identify which of the strain parts need the improvement.

Next, we compared our numerical results for the resistance time with the predictions of the European building code Eurocode 2 (2002). For the clamped column, our method predicted the resistance time 214 min for the partially insulated column, and 212 min for the uninsulated one. This is very close to the experimentally found value 208 min. By contrast, the Eurocode predicted much shorter resistance time, 181 min, when the set of simply supported columns was studied in our second numerical example. We found that Eurocode 2 predicted about 10% longer resistance time than calculated with our method. This is a surprise, because standards are assumed to give conservative, the safe side results. Only further systematic and well documented experimental analyses could resolve the question if this is indeed so.

References

Anderberg, Y., Thelandersson, S., 1976. Stress and Deformation Characteristics of Concrete at High Temperatures, 2. Experimental Investigation and Material Behaviour Model. Lund Institute of Technology, Sweden.

ASTM E-119-76, 1976. Standard Methods of Fire Tests of Building Construction and Materials, Annual book of ASTM standards, Parts 18, American Society for Testing and Materials.

Bratina, S., Saje, M., Planinc, I., 2003a. On materially and geometrically non-linear analysis of reinforced concrete planar frames, Internal report 1/2003, University of Ljubljana, Faculty of Civil and Geodetic Engineering, Chair of Mechanics, 49p.

Bratina, S., Planinc, I., Saje, M., Turk, G., 2003b. Non-linear fire-resistance analysis of reinforced concrete beams. Structural Engineering and Mechanics 16 (6), 695–712.

Bratina, S., Saje, M., Planinc, I., 2004. On materially and geometrically non-linear analysis of reinforced concrete planar frames. International Journal of Solids and Structures 41 (6), 7181–7207.

Cai, J., Burgess, I., Plank, R., 2003. A generalised steel/reinforced concrete beam-column element model for fire conditions. Engineering Structures 25 (6), 817–833.

Cioni, P., Croce, P., Salvatore, W., 2001. Assessing fire damage to r.c. elements. Fire Safety Journal 36, 181–199.

Cruz, C.R., 1968. Apparatus for measuring creep of concrete at high temperatures. Journal of the PCA Research and Development Laboratories 10 (3), 36–42.

Dotreppe, J.-C., Franssen, J.-M., Vanderzeypen, Y., 1999. Calculation method for design of reinforced concrete columns under fire conditions. ACI Structural Journal 96 (1), 9–18.

Ellingwood, B., Lin, T.D., 1991. Flexure and shear behaviour of concrete beams during fires. ASCE Journal of Structural Engineering 117 (2), 440–458.

Eurocode 1, 1995. Basis of Design and Actions on Structures, Part 2-2: Actions on structures–Actions on structures exposed to fire, ENV 1991-2-2.

Eurocode 2, 1991. Design of Concrete Structures, Part 1: General rules and rules for buildings, ENV 1992-1-1.
Eurocode 2, 2002. Design of Concrete Structures, Part 1-2: General rules–Structural Fire Design, prEN 1992-1-2.
Franssen, J.-M., Dotreppe, J.-C., 2003. Fire tests and calculation methods for circular concrete columns. Fire Technology 39, 89–97.
Harmathy, T.Z., 1993. Fire Safety Design and Concrete. Longman, London.
Huang, Z., Burgess, I.W., Plank, J.R., 1999. Nonlinear analysis of reinforced concrete slabs subjected to fire. ACI Structural Journal 96 (1), 127–135.
Huang, Z., Platten, A., Roberts, J., 1996. Non-linear finite element model to predict temperature histories within reinforced concrete in fire. Building and Environment 31 (2), 109–153.
Lie, T.T., Celikkol, B., 1991. Method to calculate the fire resistance of circular reinforced concrete columns. ACI Materials Journal 88 (1), 84–91.
Lie, T.T., Irwin, R.J., 1993. Method to calculate the fire resistance of reinforced concrete columns with rectangular cross section. ACI Structural Journal 90 (1), 52–60.
Lin, T.D., Ellingwood, B., Piet, O., 1988. Flexural and shear behaviour of reinforced concrete beams during fire tests, PCA Research and Development Bulletin, Report No. NBS-GCR-87-536, Center for Fire Resarch, National Bureau of Standards, Washington.
Lin, T.D., Zwiers, R.I., Burg, R.G., Lie, T.T., McGrath, R.J., 1992. Fire resistance of reinforced concrete columns, PCA Research and Development Bulletin, RD101B.
Kodur, W.K.R., Wang, T.C., Cheng, F.P., 2004. Predicting the fire resistance behaviour of high strength concrete columns. Cement and Concrete Composites 26, 141–153.
Najjar, S.R., Burgess, I.W., 1996. A nonlinear analysis of three-dimensional steel frames in fire conditions. Engineering Structures 18 (1), 77–89.
Planinc, I., Saje, M., Čas, B., 2001. On the local stability condition in the planar beam finite element. Structural Engineering and Mechanics 12 (5), 507–526.
Reissner, E., 1972. On one-dimensional finite-strain beam theory: the plane problem. Journal of Applied Mathematics and Physics (ZAMP) 23, 795–804.
Saje, M., Turk, G., (1987). HEATC, Computer programme for non-linear transient heat conduction problems, University of Ljubljana, Faculty of Civil and Geodetic Engineering, Ljubljana.
Sidibé, K., Duprat, F., Pinglot, M., Bourret, B., 2000. Fire safety of reinforced concrete columns. ACI Structural Journal 97 (4), 642–647.
The MathWorks, Inc., MATLAB 1999. Natick, Available from: <http://www.mathworks.com>.
Williams-Leir, G., 1983. Creep of structural steel in fire: analytical expressions. Fire and Materials 7 (2), 73–78.
Vratanar, B., Saje, M., 1998. A consistent equilibrium in a cross-section of an elastic–plastic beam. International Journal of Solids and Structures 36, 311–337.
Zha, X.X., 2003. Three-dimensional non-linear analysis of reinforced concrete members in fire. Building and Environment 38, 297–307.
Zhao, J.-C., 2000. Application of the direct iteration method for non-linear analysis of steel frames in fire. Fire Safety Journal 35, 241–255.